AMERICAN
METEOROLOGICAL
SOCIETY

Bulletin of the American Meteorological Society

EARLY ONLINE RELEASE

This is a preliminary PDF of the author-produced manuscript that has been peer-reviewed and accepted for publication. Since it is being posted so soon after acceptance, it has not yet been copyedited, formatted, or processed by AMS Publications. This preliminary version of the manuscript may be downloaded, distributed, and cited, but please be aware that there will be visual differences and possibly some content differences between this version and the final published version.

The DOI for this manuscript is doi: 10.1175/BAMS-D-12-00160.1

The final published version of this manuscript will replace the preliminary version at the above DOI once it is available.

GPM Satellite Simulator Over Ground Validation Sites

Toshihisa Matsui[1&2], Takamichi Iguchi[1&2], Xiaowen Li[1&3], Mei Han[1&3], Wei-Kuo Tao[2], Walter Petersen[4], Tristan L'Ecuyer[5], Robert. Meneghini[1], William Olson[1&6], Christian D. Kummerow[7], Arthur Y. Hou[1], Mathew R. Schwaller[1], Erich F. Stocker[1], John Kwiatkowski[1&8]

1. NASA GSFC, Greenbelt, MD
2. University of Maryland College Park, College Park, MD
3. Goddard Earth Sciences Technology and Research, Morgan State University, Baltimore, MD
4. NASA GSFC, Wallops Flight Facility, Wallops Island, VA
5. University of Wisconsin-Madison, Madison, WI
6. University Maryland Baltimore County, Baltimore, MD
7. Colorado State University, Fort Collins, CO
8. George Mason University, Fairfax, VA

Submitted to BAMS
Nov 5, 2012
In Box Article

Corresponding Author.
Toshihisa Matsui
Code 612, NASA Goddard Space Flight Center
Greenbelt, MD
Tel: 301-614-5658
Toshihisa.Matsui-1@nasa.gov

1. The Global Precipitation Measurement (GPM) mission

The Global Precipitation Measurement (GPM) Core Observatory will be launched in February 2014 (Hou et al. 2013). It will provide next-generation satellite rainfall measurement and better understanding of energy/water cycles in the weather and climate system, after 15 years of successful operation of the Tropical Rainfall Measuring Mission (TRMM) satellite (Simpson et al. 1988). In comparison with TRMM satellite (±38° latitude), GPM will extend measurements to high latitudes (±65° latitude), where light precipitation and snowfall frequently occur over the continents. In order to meet accuracy requirements, the GPM Core satellite carries a combination of active and passive microwave sensors with improved capabilities to detect light rain and falling snow. The GPM Dual-frequency Precipitation Radar (DPR) provides radar observations at both Ku-band (13.6 GHz) (similar to TRMM Precipitation Radar), and Ka-band (35.5GHz), where the latter includes a high-sensitivity mode designed for improved detection of light/frozen precipitation. The GPM Microwave Imager (GMI) includes 10~89GHz channels (similar to the TRMM Microwave Imager) and 166~183GHz channels. These sensor upgrades require more complex precipitation algorithms that harness multi-sensor and multi-frequency satellite signals to estimate warm/cold/mixed-phase precipitation rate over various precipitation regimes.

Prior to the Core Observatory launch, the "day-one" GPM operational precipitation algorithms and their associated products must be tested using proxy data to demonstrate their validity[1]. Algorithm testing requires representative measurements of GPM-observable signals associated with geophysical parameters (e.g., precipitation rate). One approach is to use a combination of *in situ* microphysics profiles (point observation) and airborne remote sensing

[1] NASA's Earth science spaceflight missions now routinely generate geophysical data products within hours of the start of instrument operations, and public distribution usually occurs within about 6 months of launch.

data from field campaigns, but sampling deficiencies limit the broad applicability of this method. A different approach is to use a database constructed from a Cloud-System Resolving Model (CSRM[2]), and to generate synthetic data for testing. Prior to the TRMM satellite launch (1997), the Goddard Cumulus Ensemble model with bulk single-moment microphysics (Tao and Simpson 1991) was widely used for such algorithm testing purposes (e.g., Meneghini and Kozu 1990).

2. Synthetic GPM Simulator

During the GPM era, we developed the synthetic GPM simulator that integrates *in situ* observations, a CSRM, and satellite simulators to synergistically support development of the GPM precipitation algorithms. First, CSRM-simulated precipitation systems are evaluated and constrained by the *in situ* observations from various field campaigns. Second, GPM-observable signals are simulated from the CSRM-simulated geophysical parameters through the unified satellite simulators (Fig. 1). In this way, a bottom-up approach is taken to "upscale" *in situ* point measurements to CSRM scales (1 km); then to the sensor footprint scales (5~30km), and finally to the satellite swath scales (125km~ 1500km).

The GPM Ground Validation (GV) program recently conducted a series of field campaigns in mid- and high-latitude regions over Ontario, Canada [Canadian CloudSat/CALIPSO Validation Project (C3VP), the GPM Cold-season Precipitation Experiment

[2] Non-hydrostatic mesoscale atmospheric model with horizontal grid spacings less than a few kilometers.

(GCPEx)[3]], Helsinki, Finland [Light Precipitation Validation Experiment (LPVEx, L'Ecuyer et al. 2010)], and Oklahoma, USA [Midlatitude Continental Convective Clouds Experiment (MC3E)], in order to study various types of precipitation processes. In addition to the main GV field campaigns, there were the NOAA Hydrometeorology Testbed (HMT) campaign over the Sierra Nevada Mountains and the DOE Tropical Warm Pool - International Cloud Experiment[4] (TWP-ICE) near Darwin, Australia (Table 1). The observations consisted of a suite of ground-based dual-polarimetric multi-frequency radar, rain and snow gauges, disdrometers, and aircraft-based rainfall microphysics measurements (Table 2). Airborne remote sensors collected GMI/DPR-like measurements. Collectively, these ground and airborne datasets provide a set of GPM sensor-observable signals, coincident with ground-based and airborne observed rainfall rates, rain and snow size, and ice/snow bulk and particle shape characteristics. Not all of these parameters are directly retrieved via satellite remote sensing, but they are relevant to the formulation of a priori physical assumptions in algorithms. In each GV campaign, we have identified two unique "golden-day" cases that capture ideal precipitation systems with intensive observations from the deployed instruments (Table 1).

The Weather Research and Forecasting model with Spectral Bin Microphysics (WRF-SBM) is one of the most advanced CSRM designed to support the GPM satellite mission. The WRF-SBM was developed from the Advanced Research WRF version 3.1.1 and coupled with the SBM originally developed for the Hebrew University Cloud Model (*Khain et al*., 2011). In comparison with the previous CSRM simulations used in previous satellite simulator studies

[3] GCPEx cases are not included in the first version of the orbital database due to its recent conclusion, but will be included in the second version of the orbital database.

[4] TWP-ICE cases are generated from the Goddard Cumulus Ensemble Model with Spectra-Bin Microphysics.

(Tao and Simpson 1991), the WRF-SBM has a number of new features and innovations. First, the WRF core allows for heterogeneous surfaces with a terrain-following coordinate system, rather than a flat terrain common to idealized CSRMs. This enables various terrain-induced storm simulations, such as orographic precipitation or lake-effect storms. Second, the WRF core features multiple nested domains to downscale synoptic-scale analyses (50~100km) to resolve storm-scale dynamics (1-km horizontal grid spacing and 60 vertical layers). Therefore mesoscale and synoptic-scale propagating precipitation systems, such as mid-latitude convective systems, frontal systems, and high-latitude snow systems, can be simulated in addition to tropical precipitation.

Third, and most importantly, the WRF-SBM features explicit size-bin-resolving cloud microphysics rather than the bulk microphysics used in the previous TRMM algorithm CSRM support. Cloud hydrometeors are categorized into liquid droplets, ice crystals (plate, column, dendrite), snow aggregates, graupel, and hail in the SBM. The discrete particle size distributions (PSDs) of the hydrometeor classes are represented by 43 bins covering a large range of particles sizes, unlike the fixed-shape PSDs in bulk microphysics schemes. The melting and riming processes are also explicitly calculated for each snow aggregate size bin (*Khain et al.*, 2011; *Iguchi et al.* 2012a and 2012b), allowing for a natural transition between hydrometeor species rather than the spontaneous conversion used in more common bulk microphysics formulations.

Because of its complexity, the WRF-SBM demands an order of magnitude greater computational resource than the WRF using a bulk microphysics scheme. We have conducted and stored several testbed cases with the WRF-SBM on the Pleiades supercomputer, operated by

the NASA Advanced Supercomputing division in the NASA Ames Research Center. A 24-hr WRF-SBM simulation generally requires ~5000 processors and ~2 TB storage for hourly output data. With such computational power, the WRF-SBM can provide more detailed microphysics (PSDs, effective density, melt fraction) information at higher resolution (1-km horizontal grid spacing) and over a larger area (~250,000km^2) than the idealized CSRM used in the TRMM pre-launch era (Tao and Simpson 1993). The accuracy of the simulations with the bin microphysics scheme will be improved by incorporating various constraints derived from detailed GV observations.

GV-constrained WRF-SBM. The procedure to establish a GV-constrained WRF-SBM system includes a number of steps. First, a time series of simulated three-dimensional radar reflectivity of weather radar is computed from the WRF-SBM, and the instantaneous macro-structure of precipitation systems is evaluated by comparing the spatial and temporal variability of the simulated reflectivity to observations from the operational weather radar. During this evaluation step, the lateral and surface boundary forcing (analysis) or initial conditions of the WRF-SBM simulation are modified for forecast improvement.

Second, the statistical properties of the simulated radar echoes, such as the echo-top height and the maximum intensity in the column are evaluated. These statistical parameters can be used to help validate the WRF-SBM-simulated microphysics profiles. Additional properties of the PSDs such as hydrometeor effective densities and terminal velocities are further evaluated against the aircraft- and ground-based *in situ* measurements (Table 2). The individual measurement specifications of the *in situ* instruments are implemented to compute instrument-

equivalent parameters from the WRF-SBM through the guidance from GV scientists. This software module, the *GV simulator*, is a newly developed component in the Synthetic GPM Simulator [see examples in Iguchi et al. (2012a)].

Based upon results from the detailed microphysics evaluation, we modify microphysics process parameters, such as the number of background aerosols, ice nuclei, ice collision and coalescence rate, amount of super cooled water, to name some, in order to bring the model fields into alignment with the observations [see more details in Iguchi et al. (2012a; 2012b)].

The GPM satellite simulator translates the WRF-SBM-simulated geophysical parameters into the GPM-observable L1B [raw instrumental signals: microwave brightness temperature (Tb) for the GMI and equivalent radar reflectivity factor (Zm) for the DPR] signals in an orbital format (Fig 2). The GPM satellite simulator has been built upon the existing multi-sensor satellite simulator, the Goddard Satellite Data Simulator Unit (G-SDSU) (Matsui et al. 2009), which is the spin-off version of the SDSU (Masunaga et al. 2011). The G-SDSU integrates several independent Fortran modules: *the IO Module*, *the Optics Module*, *the Surface Module*, *the Radiative Transfer Modules*, *the Radar Module*, and, the recently developed *Scan Module*. This Fortran-based package of modules constitutes a comprehensive end-to-end GPM satellite simulator. Brief explanations of the most important modules are included here.

First, instantaneous fields of PSD bins, melting/riming fraction, atmospheric profile (temperature, pressure, humidity), and surface parameters (surface elevation, surface type, geolocation) are incorporated from the WRF-SBM simulation into *the IO Module*. Due to the

enormous file size of the WRF-SBM, the G-SDSU decomposes the WRF-SBM domains into small sub-domains for each CPU and its memory through Message Passing Interface processing.

Second, using the center location of the WRF-SBM domain, *the Scan Module* calculated satellite track and instrument-specific field-of view (FOV). The satellite track is estimated via the Keplerian orbit and Kozai's 1st order perturbation theory (Kidder 2002). Then, orbit parameters and satellite sensor scanning system/geometry (GMI imager/sounder and DPR Ku/Ka bands) are used to calculate time progress of FOV geolocation, sensor incident angles, and antenna gain functions for each instrument sampling (Fig 2).

Third, particle single-scattering properties are computed at each WRF-SBM grid point via Lorenz-Mie method in *the Optics Module*. Effective refractive indices are computed through the Maxwell-Garnett method that accounts for bin-by-bin particle effective density (riming fraction) and melting fraction. Single-particle single-scattering properties are integrated over the explicit PSD and over the various species to represent bulk single-scattering properties. *The Surface Module* predicts land- and ocean-surface emissivity. Land-surface emissivity is computed from the *Tool to Estimate Land-Surface Emissivities at Microwave frequencies* (TELSEM: *Aires et al.* 2011), while water-surface emissivity is a function of salinity, wind speed, and temperature (Wilheit 1979).

For the GMI sensor, top-of-atmosphere microwave Tbs are computed via the two-stream model with Eddington's Second Approximation (*Kummerow* 1993) using bulk single-scattering properties along FOV-satellite slant paths in *the Radiative Transfer Module*. This slant-path

approach mimics rigorous 3D microwave radiative transfer approach by using a 1D radiative transfer model (*Olson et al.* 2001). This module also considers the effect of terrain. Computed microwave Tbs are convolved over the antenna gain functions to represent measurements of brightness temperature over the footprint, called the Effective Field of View (EFOV). The EFOV describes the combined effects of the half-power beam width of the antenna gain and the radiometer sample integration period. GMI beam widths of the high- to low- frequency channels range from 0.4° (183 GHz) to 1.75° (10 GHz), corresponding to footprint sizes from 5 km to 30 km, respectively.

The Radar Module calculates the attenuated and attenuation-corrected equivalent radar reflectivity factors (Zm and Zt, respectively) along the FOV-satellite path. Radar range (distance between radar returns and satellite positions) is estimated from the *Scan Module*. Zm and Zt are averaged over the individual pulse volumes using the Gaussian antenna gain pattern. In this process, terrain effects on radar sampling volume or area are used to account for the influence of surface clutter effects in the cross-track scanning radar. At the radar range just above the surface, the total two-way path-integrated attenuation is estimated. Multiple scattering effects are not yet considered in the Radar Module. The vertical and horizontal sampling strategy in *the Radar Module* follows the GPM DPR algorithm (*Iguchi et al.* 2010).

Simulated Orbital GPM Testbed consists of satellite orbital parameters, the GMI Tbs, and the DPR reflectivities. A total of 240 scenes of orbital data were generated from ten GV cases for supporting GPM pre-launch algorithm development. Fig 3 displays simulated GMI Tb and DPR reflectivity from a selected scene of each site. The panel shows diverse spectrum of

simulated GPM satellite signals associated with different precipitation systems; however, the orbital database is limited over the WRF-SBM regional domain instead of an entire single orbit. The uniqueness of this simulated orbital data is the inclusion of the detailed retrieval-like geophysical parameters derived from the WRF-SBM, such as rainfall rate, column water vapor, surface skin temperature, and moments of precipitation PSDs. These geophysical parameters are also processed with the same antenna convolution method as is done in the GMI and DPR modules. Thus, the satellite sensor-observable signals and algorithm-retrievable geophysical parameters are sampled in identical footprints within the same dataset, allowing algorithm scientists to quickly assess their retrieval algorithm products.

For convenience, the NASA Precipitation Processing System team converts the simulator output into the format adopted for the official GPM satellite products. The initial version (V1) of the synthetic orbital dataset is available at the ftp sites[5]. The official product can be readily visualized and checked by the new GPM-era free viewer THOR (the Tool for High-resolution Observation Review[6]). The original WRF-SBM database is also available through the NASA GSFC Cloud Library[7].

3. Future Directions

The GPM simulator utilizes improved observations, CSRMs and satellite simulators compared to those used in the earlier TRMM pre-launch era. The comprehensive combination of detailed storm scenes with *in situ* data constraints and realistic forward models perhaps has not

[5] HDF version is available in ftp://trmmopen.gsfc.nasa.gov/pub/simulatedData/, while NetCDF version is available in ftp://gpm.nsstc.nasa.gov/gpm_validation/related_projects/simulated_orbits/.

[6] THOR is available at http://pps.gsfc.nasa.gov/tsdis/THOR/release.html

[7] http://cloud.gsfc.nasa.gov/index.php?section=15

been previously achieved in other simulated datasets (Meneghini and Kozu 1990; Grasso et al. 2008). Further improvement of the WRF-SBM simulations and the GPM satellite simulator is planned in the near future. Version 2 of the orbital database will feature a full upgrade of particle single scattering databases from the Lorenz-Mie method (spherical assumptions in particle shapes) to the Discrete-Dipole Approximation (Draine and Flatau 1994) and T-matrix methods (Mishchenko et al 1996) to account for the effects of complex structures of snow particles as observed from existing satellite measurements and polarimetric ground-based radar measurements. Microphysics of the WRF-SBM simulation will be further evaluated and improved upon the GV measurements. After the launch of the GPM Core satellite, the GPM satellite simulator will be a useful tool for radiance-based precipitation microphysics evaluation and assimilation methods (e.g., *Matsui et al.* 2009, *Li et al.* 2010, *Han et al.* 2013; *Zupanski et al.* 2011) using the GPM measurements.

Acknowledgement. The project is funded by the NASA Precipitation Measurement Mission (PMM) program (NNX11AR17G). The authors are grateful to Dr. R. Kakar at NASA HQ for his support of this research, and also thank to the NASA Advanced Supercomputing (NAS) Division in the NASA Ames Research Center. We also thanks to many GV scientists, who provided us useful datasets.

For Further Reading

Aires, F., C. Prigent, F. Bernardo, C. Jiménez, R. Saunders, P. Brunel, 2011: A Tool to Estimate Land-Surface Emissivities at Microwave frequencies (TELSEM) for use in numerical weather prediction, *Quarterly Journal of the Royal Meteorological Society*, **137**(656), 690–699.

Draine, B., and P. Flatau, 1994: Discrete-dipole approximation for scattering calculations. *Journal of the Optical Society of America A*, **11,** 1491-1499.

Grasso, L., M. Sengupta, J. Dostalek, R. Brummer, M. Demaria. (2008), Synthetic satellite imagery for current and future environmental satellites. *International Journal of Remote Sensing*, **29**(15), 4373-4384.

Han M., S. A. Braun, T. Matsui, C. R. Williams, 2013: Evaluation of cloud microphysics schemes in simulations of a winter storm using radar and radiometer measurements, *Journal of Geophysics Research*, doi:10.1029/2012JD018301.

Hou, A. Y., R. Kakar, S. Neeck, A. Azarbarzin, C. Kummerow, M. Kojima, R. Oki, K. Nakamura, and T. Iguchi, 2013: The Global Precipitation Measurement (GPM) Mission. *Bulletin of American Meteorological Society*, (Submitted).

Iguchi, T. S. Seto, R. Meneghini, N. Yoshida, J. Awaka, T. Kubota, 2010: GPM/DPR Level-2 Algorithm Theoretical Basis Document, available online (http://pps.gsfc.nasa.gov/atbd/atbd.html).

Iguchi, T., T. Matsui, J. J. Shi, W.-K. Tao, A. P. Khain, A. Hou, R. Cifelli, A. Heymsfield, and A. Tokay, 2012: Numerical analysis using WRF-SBM for the cloud microphysical structures in the C3VP field campaign: Impacts of supercooled droplets and resultant riming on snow microphysics. *Journal of Geophysical Research*, **117**, D23206, doi:10.1029/2012JD018101.

Iguchi, T., T. Matsui, A. Tokay, and P. Kollias, and W.-K. Tao, 2012b: Two distinct modes seen in one-day rainfall event on the MC3E field campaign: Analyses of disdrometric data and WRF-SBM simulation, *Geophysical Research Letteters*, **39**, L24805, doi:10.1029/2012GL053329.

Khain, A., A. Pokrovsky, D. Rosenfeld, U. Blahak and A. Ryzhkov, 2011: The role of CCN in precipitation and hail in a mid-latitude storm as seen in simulations using a spectral (bin) microphysics model in a 2D dynamic frame, *Atmospheric Research*, **99**, 129-146.

Kidder, S. Q., 2002: Satellites: Orbits, in J. R. Holton, J. Pyle, and J. A. Curry, (eds.), *Encyclopedia of Atmospheric Sciences*, Academic Press, 2024-2038.

Kummerow, C., 1993: On the accuracy of the Eddington approximation for radiative transfer in the microwave frequencies. *Journal of Geophysical Research*, **98**, 2757-2765.

L'Ecuyer, T. W. Petersen, and D. Moiseev, 2010: Light Precipitation Validation Experiment (LPVEx), http://lpvex.atmos.colostate.edu/docs/lpvex_science_plan_June2010.pdf

Li, X., W.-K. Tao, T. Matsui, C. Liu, and H. Masunaga, 2010: Improving a spectral bin microphysical scheme using long-term TRMM satellite observations. *Quarterly Journal of Royal Metrological Society*, **136**(647), 382-399.

Masunaga, H., Matsui, T., W.-K. Tao, A. Y. Hou, C. Kummerow, T. Nakajima, P. Bauer, W. Olson, M. Sekiguchi, and T. Y. Nakajima, 2010: Satellite Data Simulation Unit: Multi-Sensor and Multi–Frequency Satellite Simulator package, *Bulletin of American Meteorological Society*, **91**, 1625-1632.

Matsui, T., X. Zeng, W.-K. Tao, H. Masunaga, W. Olson, and S. Lang, 2009: Evaluation of long-term cloud-resolving model simulations using satellite radiance observations and

multifrequency satellite simulators. *Journal of Atmospheric and Oceanic Technology*, **26**, 1261-1274.

Meneghini, R. and T. Kozu, 1990: Spaceborne Weather Radar, Artech House. 212p.

Mishchenko, M., L. Travis, and D. Mackowski, 1996: T-matrix computations of light scattering by non-spherical particles: A review. *Journal of Quantitative Spectroscopy and Radiative Transfer*, **55,** 535-576.

Olson, W. S., P. Bauer, C. D. Kummerow, Y. Hong, W.-K. Tao, 2001: A melting-layer model for passive/active microwave remote sensing applications. Part II: simulation of TRMM observations. *Journal of Applied Meteorology*, **40**, 1164–1179.

Simpson, J., R. F. Adler, G. R. North, 1988: A Proposed Tropical Rainfall Measuring Mission (TRMM) Satellite. *Bulletin of American Meteorological Society*, **69**, 278–295.

Wilheit, T. T., 1979: A model for the microwave emissivity of the ocean's surface as a function of wind speed. *IEEE Trans. Geosci. Electron.,* **GE-17,** 244–249.

Zupanski, D., S. Q. Zhang, M. Zupanski, A. Y. Hou, S. H. Cheung, 2011: A rrototype WRF-based ensemble data assimilation system for dynamically downscaling satellite precipitation observations. *Journall of Hydrometeorology*, **12**, 118–134.

Site Name	Location	Date	Details of Precipitation Systems
C3VP (Canadian CloudSat/CALIPSO Validation Project)	Ontario Canada	1/19/2007	Lake-effect snow breeze. Narrow and shallow snow band.
		1/21/2007	Large-scale homogeneous storm event.
LPVEx (Light Precipitation Validation Experiment)	Helsinki Finland	9/21/2010	Large-scale mixed-phase stratiform rain with relatively high (~2400m) altitude of melting band.
		10/20/2010	Large-scale mixed-phase stratiform rain with low (~1000m) altitude of melting band.
MC3E (Midlatitude Continental Convective Clouds Experiment)	Oklahoma USA	4/25/2011	Multi-cell MCS and shallow stratiform rain.
		5/20/2011	Severe convection and extensive stratiform rain.
TWP-ICE (Tropical Warm Pool - International Cloud Experiment	Darwin Island, Australia	1/23/2006	Propagating organized tropical convection.
		2/05/2006	Isolated cumulus congestus.
HMT (Hydrometeorology Testbed)	California, USA	12/30/2005	Frontal orogenic mixed-phased rainfall (matured).
		12/31/2005	Frontal orogenic mixed-phased rainfall (decaying).

Table 1. Description of GPM Ground Validation (GV) sites and additional sites, locations, golden cases, and precipitation systems.

GV measurements		
Instruments		Measurable
Ground	Weather Radar	Three-dimensional C-band radar image
	NASA Polarimetric (NPOL) radar	S-band radar image and polarimetric parameters
	Vertical Pointing S-, Ku, W-band radar	Times series of reflectivity and Doppler velocity profiles
	2 Dimensional Video Disdrometor (2DVD)	Particle shape information
		Terminal velocity
		Rain rate (volumetric rate for snowfall)
	Particle Size and Velocity (PARSIVEL) Disdrometer	Bulk particle size distributions (PSDs), number concentrations
		Spectrum bulk terminal velocity
		Rain rate (volumetric rate for snowfall)
	Geonor Bucket	Rain rate (melted rain rate for snowfall)
Aircraft	W-band cloud radar	W-band radar reflectivity and Doppler velocity
	The Compact Scanning Millimeter-wave Imaging Radiometer (CoSMIR), Advanced Microwave Precipitation Radiometer (AMPR)	GMI-like microwave brightness temperature
	High-Altitude Imaging Wind and Rain, Airborne Profiler (HIWRAP)	DPR-like Ka-Ku radar reflectivity and Doppler velocity profiles
	Particle Measuring Systems (PMS) 2D-C and 2D-P	Particle 2D images
		Bulk PSDs, number concentrations
	Counterflow Virtual Impactor (CVI), Nevzorov Hot Wire probe	Bulk water content (melted amount for solid particles)
	Rosemont Icing Probe (RICE)	Voltage signals for presence of super-cooled liquid water

Table 2. Description of measurements and instruments deployed at the GPM Ground Validation (GV) sites. These data are used to evaluate the WRF-SBM.

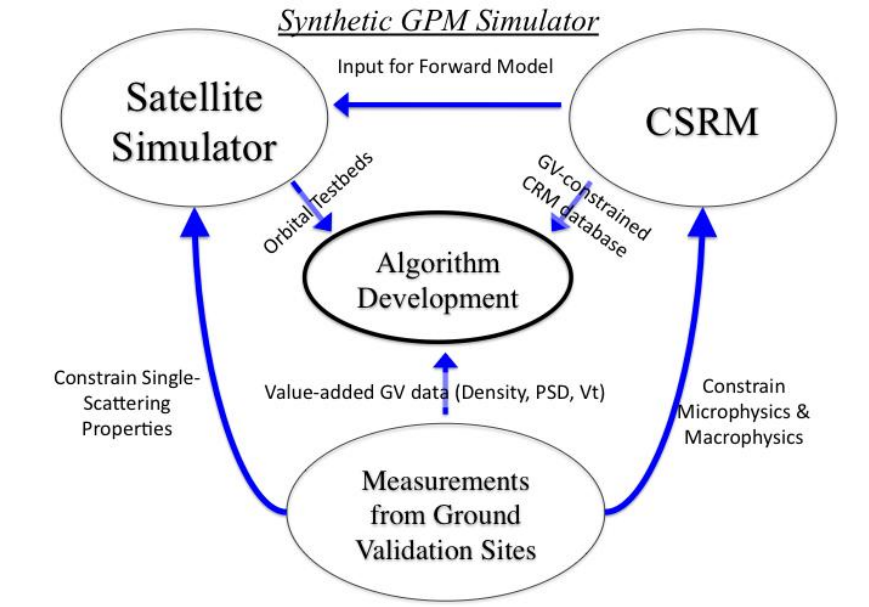

Figure 1. Framework of the synthetic GPM simulator.

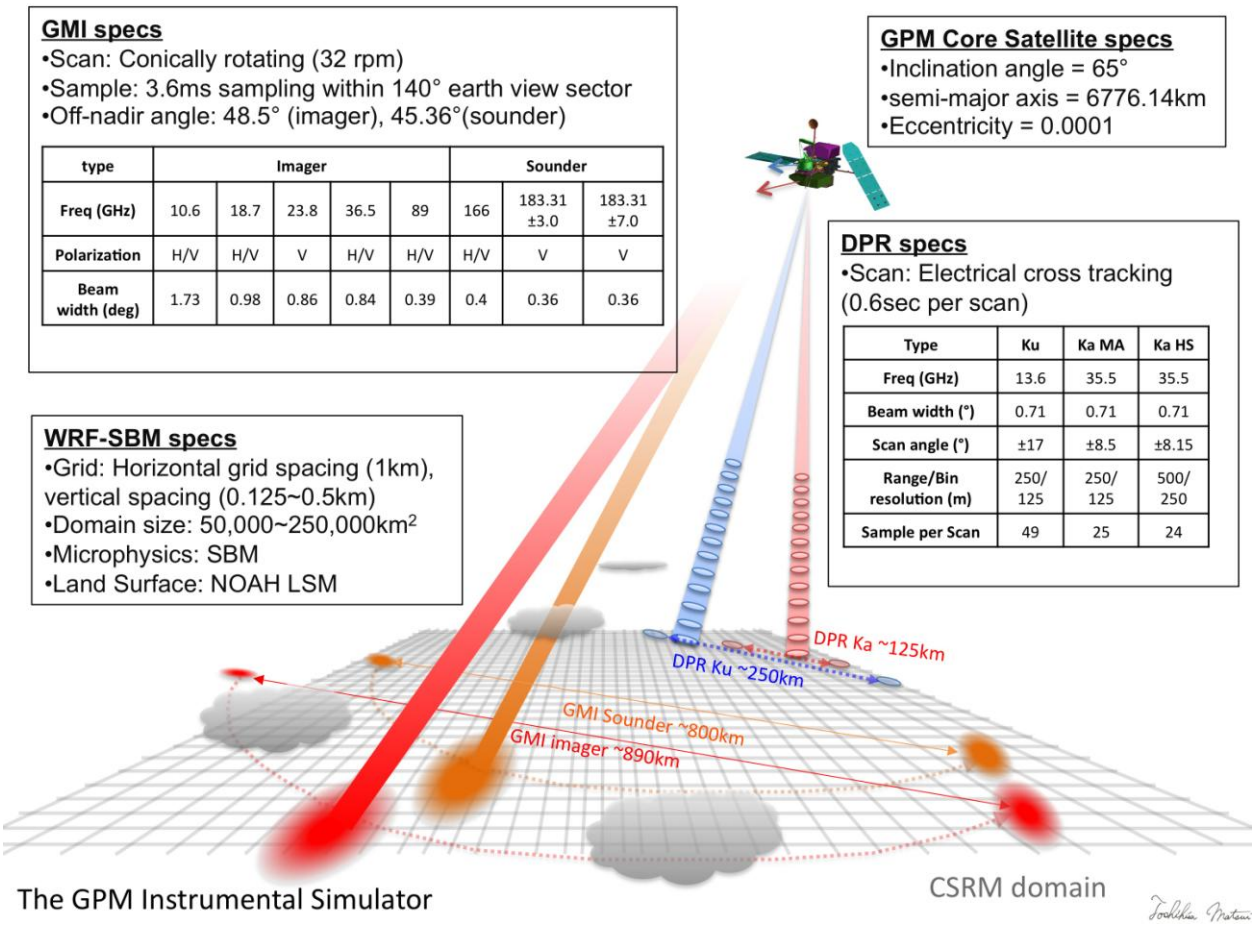

Fig 2. Schematics of the GPM satellite simulator and the specifics of the GPM Core Observatory. Note that the swath widths vary slightly at different latitudes due to the Earth's oblateness.

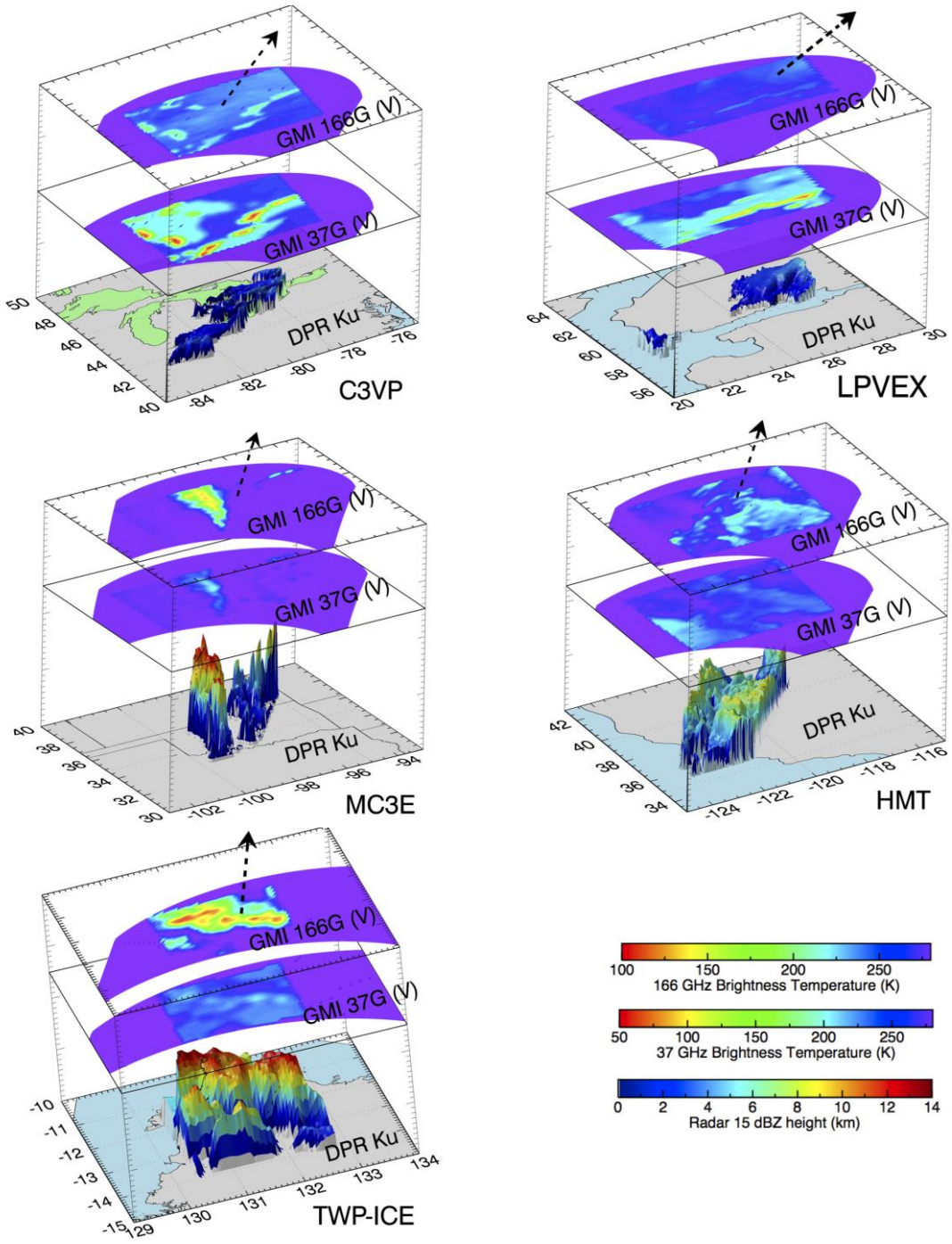

Figure 3. Three-dimensional view of the simulated GPM orbital data over selected simulation scenes from C3VP, LPVEX, MC3E, HMT, and TWP-ICE. Color-shaded terrain represents 15dBZ echo-top height of the DPR Ku band, and horizontal slices of color shades represent microwave brightness temperature of the GMI 37GHz (V) and 166GHz(V) channels.